CrossMark

RESEARCH PAPER

Simulation of Unenhanced Electrokinetic Process for Lead Removal from Kaolinite Clay

Gholamreza Asadollahfardi[1] · Milad Rezaee[1] · Gholamhosein Tavakoli Mehrjardi[1]

Abstract This paper presents a numerical model based on explicit finite difference method for contaminants transport under electrokinetic remediation process. The effect of adsorption, precipitation and water auto-ionization reactions was considered with a set of algebraic equations. Also the effect of electrolysis reaction in anode and cathode cells was considered with appropriate boundary conditions. The model predictions are compared with experimental results of electrokinetic lead removal from kaolinite in the literature. The coefficient of determination and index of agreement between the lead concentration of experimental result and model prediction were 0.974 and 0.884, respectively. The coefficient of determination and index of agreement between the pH value of experiment and the pH prediction were 0.975 and 0.976, respectively.

Keywords Finite difference · Electrokinetic · Lead · Kaolinite · Sensitivity analysis

1 Introduction

Heavy metals, organic pollutant and radionuclides are the common pollutants in the soil. Decontamination of contaminated soils with heavy metals and radionuclides is a great concern in several countries [1]. For remediation of polluted soil, different methods exist. Some of these methods are (1) bioremediation, (2) thermal remediation, (3) soil vapor extraction, (4) soil washing, (5) soil

flushing, and (6) electrokinetic remediation (EKR) [2]. Biological remediation which has been mainly used to detoxify organic contaminants [3] and soil washing, soil flushing, and EKR are mainly used for heavy metal pollutant [2]. In EKR, the contaminants transportation is due to the different physical phenomenon, including electromigration, electroosmosis, electrophoresis, and diffusion. Ionic contaminant transport to anode and cationic contaminant transport to cathode [4]. The EKR method has advantages: (1) flexibility to use as ex situ or in situ methods, (2) applicability to low-permeability and heterogeneous soils, (3) applicability to saturated and unsaturated soils, (4) applicability for heavy metals, radionuclides, and organic contaminants, as well as in any of their combinations [5]. Because of these advantages, uses of this method are extended worldwide. For understanding the fundamental of EKR process, some mathematical studies have been proposed. Alshawabkeh and Acar [6] introduced model to remediate lead. They considered the chemical reactions (water auto-ionization, precipitation and adsorption) using set of algebraic equations and they stated their model presented good results. Haran et al. [7] developed model for transport hexavalent chromium in sandy soil and ignored the term of electro-osmosis because of low surface charge of soil. Jacobs et al. [8] used numerical method to simulate remediation of soil contaminated with zinc. They considered retardation term to include adsorption and precipitation reactions and they stated that their model is in excellent agreement with experimental results. Kim et al. [9] developed model for cadmium removal using EKR process and also Kim et al. [10] generated another model for lead polluted soil. In both models, they considered the effect of chemical reactions by set of algebraic equations; however, they assumed constant electric field in their

✉ Gholamreza Asadollahfardi
fardi@khu.ac.ir; asadollahfardi@yahoo.com

[1] Department of Civil Engineering, Kharazmi University, Tehran, Iran

Springer

model for simplicity and reached good results. Park et al. [11] studied the process of EKR on phenol-contaminated kaolinite and in their work they introduced equations for counting proton and hydroxyl ions concentration in anode and cathode cells as boundary conditions. Hafiz Ahmad [12] presented experimental tests of EKR and modeled the copper transport in soil based on one of his test. He did not consider the chemical reaction except electrolysis in anode and cathode cells and adsorption with retardation factor. Vereda-Alonso et al. [4] presented model for two-dimensional EKR of copper spiked kaolin. Their model was based on Kirchoff's laws of electricity to calculate the voltage drop distribution and assuming local equilibrium conditions within the compartments. They could obtain good agreement between experimental results and prediction. Mascia et al. [13] modeled EKR of cadmium with electroneutrality assumption and considered surface reactions and they reached good result. Al-Hamdan and Reddy [14] presented a model for removing cadmium, chromium and nickel from kaolinite with assuming electroneutrality condition coupled with chemical equilibrium reactions and their model could predict the experiment reasonably. Yeung et al. [15] modeled decontaminating lead from two kinds of kaolinite (Georgia, Milwhite) by EKR method and they indicated that their model was in good agreement with experimental measurements.

This paper presents a numerical model for unenhanced EKR process based on explicit finite difference method (FDM). The effect of electrolysis reaction in anode and cathode cells, adsorption, precipitation, and water auto-ionization reactions is considered. Sensitivity analysis on retardation factor, electric field and tortuosity factor was deliberated.

2 Materials and Methods

In our model, we considered the following assumptions: (1) one dimensional, (2) isothermal conditions, (3) electrophoresis neglected, (4) the saturated porous medium, (5) kaolinite surface is negatively charged, (6) electric field assumed constant during simulation, (7) using Nernst–Einstein equation for calculating ionic mobility of species [6, 8, 10, 11].

2.1 Transport Equation

The advection–dispersion equation has been used to describe solute transport in porous media [16]. Different transport phenomena exist in EKR which considered in the present mode: (1) advection pore fluid due to electro-osmosis flow; (2) diffusion due to concentration gradients; and (3) electro-migration due to the ionic mobility of

charged ions. Based on Helmholtz–Smoluchowski (H–S) theory, which describes the flux of fluid under electric field, electro-osmosis flux is [7–9]:

$$J_{\text{eo}} = -k_{\text{eo}} \frac{\partial \emptyset}{\partial x} \tag{1}$$

where k_{eo} (m^2 V^{-1} s^{-1}) is the electro-osmosis permeability coefficient, which is the function of zeta potential and viscosity of fluid, porosity and electrical permittivity of the soil medium and $\emptyset$ (V) is the electrical potential. The formulation of k_{eo} was generated by Mitchell [17] and Eykholt and Daniel [18]:

$$k_{\text{eo}} = n \frac{\varepsilon \zeta}{\mu} \tag{2}$$

where μ (C V s m^{-3}) is the viscosity of fluid, n (–) is the porosity of soil medium, ε (F m^{-1}) is the permittivity of the medium and ζ (V) is the zeta potential. The zeta potential is the function of pH of soil medium; however, in a number of studies, zeta was assumed constant [6, 8–10, 19]. The relationship between zeta potential and pH was evaluated by the empirical work of Lorenz [20]:

$$\zeta \, (\text{mV}) = -38.6 + 281 e^{-0.48\text{pH}}. \tag{3}$$

Equation (4) describes the flux of ion migration which is the major transport process for ionic contaminants [5]:

$$J_i^{\text{em}} = u_i^* c_i \left(-\frac{\partial \emptyset}{\partial x} \right) \tag{4}$$

where J_i^{em} (mol m^2 s^{-1}) is the mass flux because of ion migration of the ith chemical species, c_i (mol m^3) is the concentration of specific ion, and u_i^* (m^2 V^{-1} s^{-1}) is the effective ionic mobility of specific ion.

$$u_i^* = n\tau u_i \tag{5}$$

where n (–) is the porosity of soil medium, τ (–) is the tortuosity factor and u_i (m^2 V^{-1} s^{-1}) is the ionic mobility of the specific ion that was estimated by Nernst–Einstein relation [21]:

$$u_i = \frac{D_i |z_i| F}{RT} \tag{6}$$

where D_i (m^2 s^{-1}) is the diffusion coefficient, z_i is the charge of ith chemical species, F (96485 C mol^{-1}) is the Faraday's constant, R (8.3144 J K^{-1} mol^{-1}) is the universal gas constant, and T is the absolute temperature.

The flux because of chemical gradient is described by Fick's first law of diffusion:

$$J_i^{\text{d}} = D_i^* \left(-\frac{\partial c_i}{\partial x} \right) \tag{7}$$

where J_i^{d} (mol m^{-2} s^{-1}) is the mass flux of the specific ion because of diffusion, D_i^* (m^2 s^{-1}) is the effective diffusion

coefficient of the specific ion. Effective diffusion coefficient in a porous medium has relation with the diffusion coefficient [21, 22]:

$$D_i^* = n\tau D_i \tag{8}$$

Then, the total mass flux because of the applying electric field in saturated porous media of soil is

$$J_i = D_i^* \nabla(-c_i) + c_i(u_i^* + k_{eo})\nabla(-\emptyset) \tag{9}$$

Using the mass conservation law, the partial differential equation (PDE) that describes the transport of mass in porous media of soil under electric field is evaluated:

$$n\frac{\partial c_i}{\partial t} = D_i^* \frac{\partial^2 c_i}{\partial x^2} + (u_i^* + k_{eo})\frac{\partial c_i}{\partial x}\frac{\partial \emptyset}{\partial x} + (u_i^* + k_{eo})c_i\frac{\partial^2 \emptyset}{\partial x^2} \\ - nR_i \tag{10}$$

With assuming constant electric field during the simulation, therefore, Eq. (10) leads to Eq. (11) [8–10, 12, 13]:

$$n\frac{\partial c_i}{\partial t} = D_i^* \frac{\partial^2 c_i}{\partial x^2} + (u_i^* + k_{eo})\frac{\partial c_i}{\partial x}\frac{\partial \emptyset}{\partial x} - nR_i. \tag{11}$$

$$R_i = R_i^{ad} + R_i^{p} + R_i^{aq} \tag{12}$$

Equation (12) describes the chemical reaction which consists of three parts: the first one is the adsorption reaction because of negative surface charge of clay particle, the second one is the precipitation reaction and the third one is the aqueous phase reaction.

2.2 Adsorption Reaction

Adsorption reaction for lead and proton is interactive when pH value is the effective parameter in adsorption species on soil. Alshawabkeh and Acar [6] used the empirical data of Yong et al. [23] for the lead adsorption isotherms at different pH values and concentration. Cao [24], Kim et al. [9], and Kim et al. [10] used the procedure of Alshawabkeh and Acar [6] to consider the adsorption process. For considering lead adsorption isotherm as a function of pH of the soil medium, we used the empirical relation of Yong et al. [23], in which Fig. 1 indicates the experimental result of lead adsorption in their experiments.

For proton adsorption, we did not use pH-dependent adsorption; therefore, constant retardation factor during the simulation was considered [6, 8–10].

$$\frac{c_i^*}{c_i} = K_{di} \tag{13}$$

$$R_{di} = 1 + \frac{\rho K_{di}}{n} \tag{14}$$

$$nR_{di}\frac{\partial c_i}{\partial t} = D_i^{eff}\frac{\partial^2 c_i}{\partial x^2} + (u_i^{eff} + k_{eo})\frac{\partial c_i}{\partial x}\frac{\partial \emptyset}{\partial x}; \quad i = 1, 2, \ldots, N \tag{15}$$
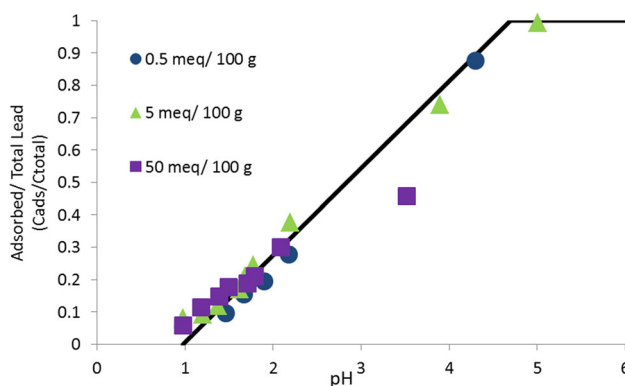

Fig. 1 Experimental result of lead linear adsorption isotherm onto kaolinite in different pH values [21]

where c_i^* (mol kg^{-1}) is the amount of solute absorbed/adsorbed onto a unit weight of solid, c_i (mol m^{-3}) is the concentration of solute, K_{di} (m^3 kg^{-1}) is the distribution coefficient, ρ (kg m^3) is the bulk dry density of the soil and R_{di} is the dimensionless retardation factor. Equation (15) represents the transport of ith species with considering retardation factor.

2.3 Precipitation Reaction

Equations (16)–(18) indicate the hydroxide and lead precipitation reaction.

$$Pb(OH)_2 \leftrightarrows Pb^{2+} + 2OH^- \tag{16}$$

$$C_{OH}^2 C_{Pb} \leq K_{sp}^{Pb(OH)_2} = 1.2 \times 10^{-15} \tag{17}$$

$$(C_{OH} - 2\Delta C)^2 \times (C_{Pb} - \Delta C) \leq K_{sp}^{Pb(OH)_2} \tag{18}$$

where $K_{sp}^{Pb(OH)_2}$ (mol L^{-1}) is the solubility product of the reaction and ΔC is the amount of ion participated in the precipitation reaction.

2.4 Aqueous Reaction

For considering aqueous reaction, we considered water auto-ionization reaction in the process. Water auto-ionization reaction is described by

$$[H^+ + x_w][OH^- + x_w] = K_w \tag{19}$$
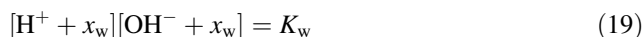
where K_w (mol L^{-1}) is the water equilibrium constant, and x_w is the meaningful root of this reaction.

$$x_w = \frac{-([H^+] + [OH^-]) + \sqrt{([H^+] + [OH^-])^2 - 4([H^+][OH^-] - K_w)^2}}{2} \tag{20}$$

where x_w describes the number of water molecules

dissociate (if $x_w > 0$) and the number of water molecules create (if $x_w < 0$) [19]. Equations (21) and (22) indicate the concentration of proton and hydroxyl after equilibrium.

$$[H^+]_{eq} = [H^+] + x_w \tag{21}$$

$$[OH^-]_{eq} = [OH^-] + x_w \tag{22}$$

3 Experimental Data

We used the data of Kim et al. [10] which was lead (II) nitrate. Figure 2 indicates the schematic diagram of their pilot test. The anode and cathode cells located on the both sides of the box and the electrolyte solution in the anode and the cathode cell were distilled water. The volume of water in anode and cathode cells was 500 mL and the dimensions of soil specimen are 10 cm × 10 cm × 15 cm with a volume of 1500 cm^3 and cross-sectional area of electrodes is 100 cm^2. Also, Table 1 indicates the experimental parameters of Kim et al. [10].
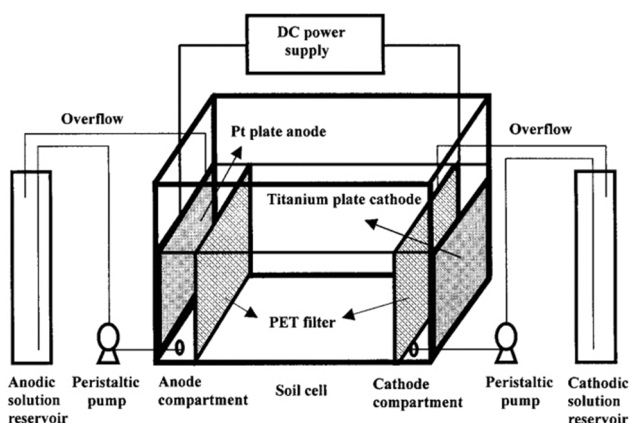

Fig. 2 Schematic diagram of experimental box [10]

Table 1 Experimental parameter of test [10]

Kaolinite clay	Type of soil
Contaminant	Lead (II) nitrate
Initial concentration of lead	7000 mg/kg
Initial soil pH	5.4
Length of soil cell	15 cm
Area of soil cell	100 cm^2
Applied current	100 mA
Applied current density	1 mA cm^{-2}
Electric potential gradient	40 V m^{-1}
Time duration	96 h
Anode electrolyte solution	Distilled water
Cathode electrolyte solution	Distilled water

4 Numerical Analysis

Equation (11) describes the ion transfer through saturated porous media of soil under electric field. The concentration of each ion such as H$^+$, OH$^-$ and Pb(II) can be obtained by solving the Eq. (11). We used explicit finite difference method (FDM), forward time and centered space (FTCS) to solve Eq. (11).

The form of the equation that was used in numerical study is

$$\frac{\partial c_i}{\partial t} = A\frac{\partial^2 c_i}{\partial x^2} + B\frac{\partial c_i}{\partial x} \tag{23}$$

where $A = \frac{D_i^*}{n}$ and $B = \frac{(u_i^* + k_{eo})\frac{\partial \phi}{\partial x}}{n}$. Therefore, the discretized form of equation is

$$\frac{c_{i,n}^{t+\Delta t} - c_{i,n}^t}{\Delta t} = A\frac{c_{i,n-1}^t - 2c_{i,n}^t + c_{i,n+1}^t}{\Delta x^2} + B\frac{c_{i,n+1}^t - c_{i,n-1}^t}{2\Delta x} \tag{24}$$

$$c_{i,n}^{t+\Delta t} = (S - 0.5C)c_{i,n}^t + (1 - 2S)c_{i,n}^t + (S + 0.5C)c_{i,n+1}^t \tag{25}$$

where $S = A\frac{\Delta t}{\Delta x^2}$, $C = B\frac{\Delta t}{\Delta x}$ and Δx and Δt are spatial and time increments, respectively. To solve each partial differential equation numerically, we introduced an initial and two boundary conditions for each species.
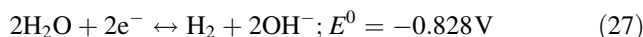
4.1 Proton (H$^+$) and Hydroxyl (OH$^-$)

Proton and hydroxyl ions are produced in anode and cathode cells due to the applying electric field.

Equation (26) describes the water oxidation reaction in anode cell:

$$H_2O \leftrightarrow \frac{1}{2}O_2 + 2H^+ + 2e^-; E^0 = -1.299\,V \tag{26}$$
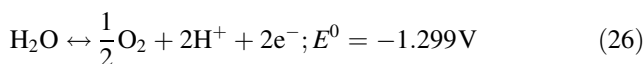
Equation (27) indicates the water reduction reaction in cathode cell:

$$2H_2O + 2e^- \leftrightarrow H_2 + 2OH^-; E^0 = -0.828\,V \tag{27}$$

We used the algebraic equation that introduced by Park et al. [11] as boundary conditions which considered the oxidation/reduction reactions in each cell. Equations (28) and (29) indicate the boundary conditions developed by Park et al. [11] that we used in our simulation. The same procedure also used by Ahmad [12]. Equations (28) and (29) are proton boundary conditions at anode and cathode cells, respectively.

$$c_{H^+} = 2K_w\left[-\frac{IA\Delta t}{FV_{reservoir}} + \left(\left(\frac{IA\Delta t}{FV_{reservoir}}\right)^2 + 4K_w\right)^{1/2}\right]^{-1} \tag{28}$$

$$c_{H^+} = \frac{1}{2}\left[-\frac{IA\Delta t}{FV_{reservoir}} + \left(\left(\frac{IA\Delta t}{FV_{reservoir}}\right)^2 + 4K_w\right)^{1/2}\right]$$

$$(29)$$

where I (A) is the current applied along the soil, A (m^2) is the cross-sectional area of the system, Δt is the time step between the new point and old point and V (m^3) is the volume of the reservoir. Hydroxyl concentration at each of anode and cathode cell could be calculated based on Eq. (30):

$$[H^+][OH^-] = K_w \qquad (30)$$

Initial concentration of proton and hydroxyl is $10^{-5.4}$ and $10^{-8.6}$ (mol L^{-1}), respectively, based on initial soil pH [10].

4.2 Lead [Pb(II)]

The initial lead concentration is 7000 mg kg^{-1} of dry soil [10]. The anode end of the soil is in contact with distilled water throughout the test. At the cathode, the concentration of water just outside the sample can be assumed equal to the concentration at the end. These boundary conditions could be expressed mathematically as [14, 25]:

$$C(0,t) = 0 \qquad (31)$$

$$\frac{\partial}{\partial x}C(L,t) = 0 \qquad (32)$$

Equations (31) and (32) indicate the lead boundary condition in soil medium in the vicinity of anode and cathode cells, respectively. Tables 2 and 3 represent the parameters used in numerical simulation and intrinsic parameter of each species, respectively. We considered proton retardation factor equal to 4.6 the value that recommended by Alshawabkeh and Acar [5]. The

Table 2 Parameters used in numerical simulation

Spatial increment length	1 mm
Time step increment	10 s
Porosity of soil (n)	0.48
Tortuosity factor (τ)	0.4
Initial electro-osmosis permeability (k_{eo})	3.66×10^{-9} m^2 V^{-1} s

electroosmosis permeability according to the Helmholtz–Smoluchowski theory is dependent mainly on the zeta potential of the soil-pore fluid interface [26] and as well zeta potential is pH dependent but in most of model which has been proposed, this parameter was kept constant equal to the initial electroosmosis permeability during the simulation [5, 8–10, 17, 22]. Therefore, we assume electroosmosis permeability constant equal to the value that Table 2 indicates.

5 Results and Discussion

Figure 3 demonstrates the pH change over time in anode and cathode cells. Oxidation reaction causes proton generation in anode and reduction reaction also causes to generate hydroxyl in cathode. As a result, the electrolyte in anode become acidify and electrolyte in cathode becomes alkaline.

Figure 4 illustrates the comparison between numerical prediction and pH measurement in the experimental test. As indicated in Fig. 4, the jump in pH near the cathode zone was occurred. This phenomenon happened because acid and base front meet each other and the sharp change was occurred in pH of the soil matrix. The pH jump is close to the cathode compartment because the ionic mobility of proton is greater than hydroxyl ionic mobility and, in addition, the electroosmosis flow direction was from anode to cathode cell. The coefficient of determination (R^2) and index of agreement (IA) between experimental results with numerical prediction were 0.975 and 0.976, respectively. Considering R^2 and IA, our prediction results are acceptable.

Figure 5 illustrates the experimental and numerical prediction of lead residual in soil. According to the linear and pH-dependent adsorption isotherm (Fig. 1), at the beginning of the test, all lead species in soil were in adsorbed form. By running the program, Proton from anode cell move to the soil medium and causes reducing pH and the adsorbed lead are able to desorb from the negative surface charge of the soil. Similar to Fig. 4, we observed a jump in lead concentrations close to cathode cell. This phenomenon causes when acid and base front meet each
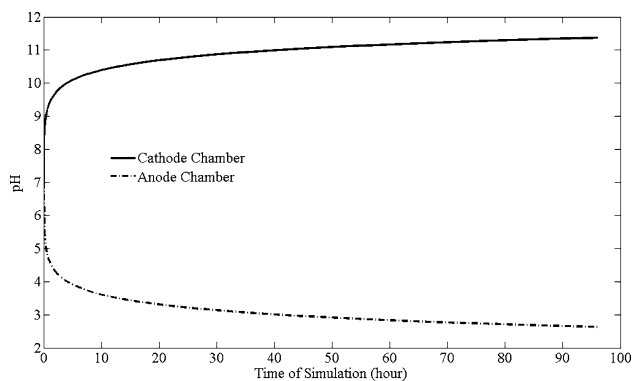
Table 3 Intrinsic parameter of each species

Species	D_i (m^2 s^{-1})[a]	u_i (m^2 V^{-1} s)[a]	D_i^* (m^2 s^{-1})[b]	u_i^* (m^2 V^{-1} s)[c]
Pb^{2+}	9.4×510^{-10}	7.36×10^{-8}	1.81×10^{-10}	1.41×10^{-8}
H$^+$	93.1×10^{-10}	36.25×10^{-8}	17.88×10^{-10}	6.96×10^{-8}
OH$^-$	52.7×10^{-10}	20.58×10^{-8}	10.12×10^{-8}	3.95×10^{-8}

[a] Extracted from Ref. [28]

[b] Calculated from Eq. (8)

[c] Calculated from Eq. (5)

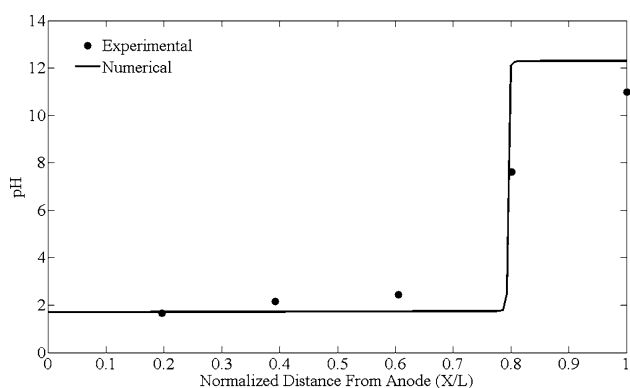**Fig. 3** pH prediction in anode and cathode chambers

Fig. 4 Comparison between the numerical prediction and the experimental results for the pH after 4 days of treatment
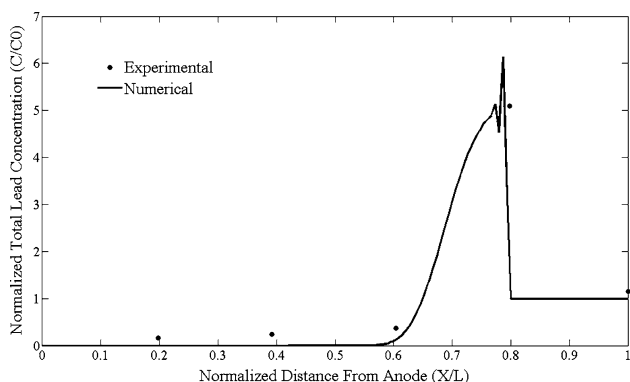

Fig. 5 Comparison between the numerical prediction and the experimental results for lead concentrations after 4 days of treatment

other and soil medium becomes alkaline and rate of adsorption and precipitation increases [5, 8, 9]. In alkaline zone, aqueous lead reacts with hydroxyl and generates the precipitated form of lead as $Pb(OH)_2$. Because of alkaline

Fig. 6 The effect of changing a retardation factor on pH prediction after 4 days of treatment

condition, high pH, aqueous lead adsorbs onto the negative surface charge of kaolinite again.

One of the most important effects of precipitation reaction near cathode is increase in the energy expenditure. Erratic precipitation of lead in alkaline region generates high resistivity zone which causes fluctuations of electrical potential difference across the electrodes. Disordered oscillation in electrical gradient increases energy expenditure [28].

As indicated in Fig. 5, the coefficient of determination (R^2) and index of agreement (IA) between the experimental results and our model prediction for lead concentration were 0.974 and 0.884, respectively. It could be concluded that our prediction is reasonable and acceptable.

6 Sensitivity Analysis

We carried out the sensitivity analysis by changing retardation factor of proton, electric field and tortuosity factor to identify the rule of each mentioned parameter. We increased or decreased each of the parameters by 20 %, while the other input parameter data were kept unchanged, then the rule of each parameter in the prediction of the lead concentration and pH was identified. Figure 6 presents the effect of changing retardation factor in the pH prediction. By increasing the retardation factor, the velocity of proton in the aqueous form was decreased and the base front progresses more in the soil medium.

Figure 7 demonstrates the result of variation of retardation factor on lead concentrations. When retardation factor was equal to 3.7, the whole soil was acidified and the rate of adsorption and precipitation decreased and lead transportation in the soil was increased and accumulated close to the cathode cell. By increasing retardation factor, the base front moves further in soil medium and alkaline condition cause to more adsorption and precipitation.
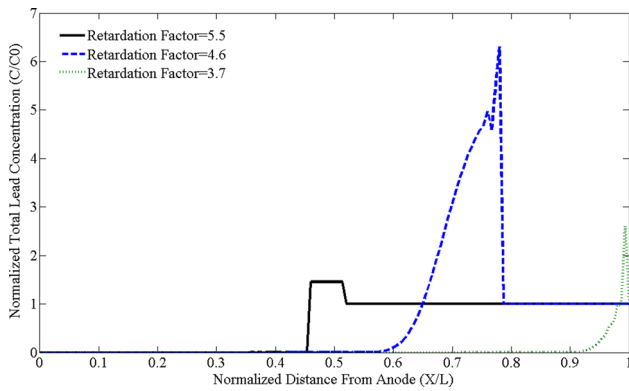
Fig. 7 The effect of changing a retardation factor on the lead prediction concentrations after 4 days of treatment
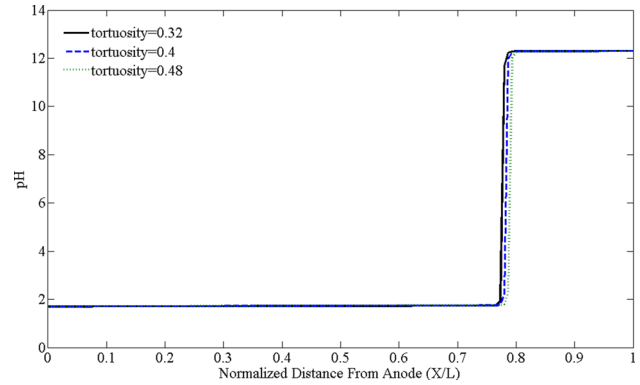

Fig. 8 The effect of changing an electrical field on pH prediction after 4 days of treatment

Fig. 9 The effect of changing an electrical field on the lead prediction concentrations after 4 days of treatment

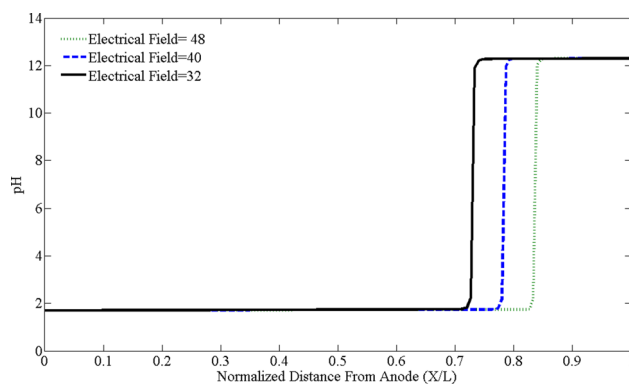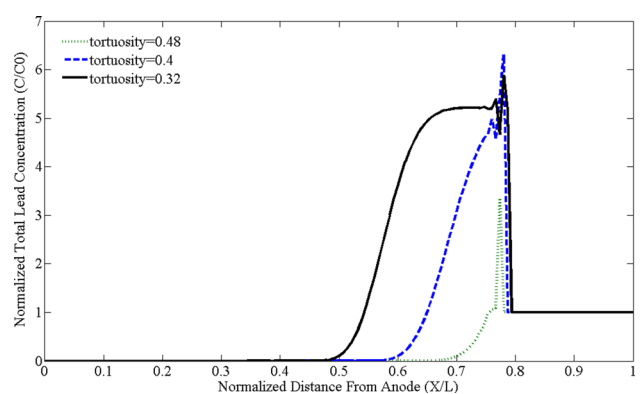**Fig. 10** The effect of changing a tortuosity factor on pH prediction after 4 days of treatment

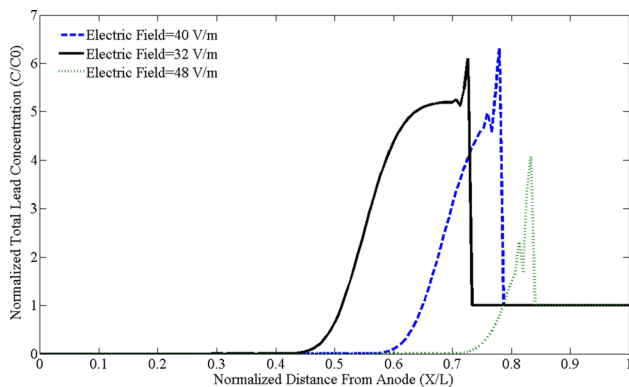**Fig. 11** The effect of changing a tortuosity factor on the lead prediction concentrations after 4 days of treatment

Figures 8 and 9 indicate the effect of different electric filed in our simulation. By increasing the electrical field (Fig. 8), the contribution of ionic-migration caused a similar effect on proton and hydroxyl transportation. However, the electroosmosis flow caused an increase in the rate of proton velocity. By increasing the electrical field (Fig. 9),

the contribution of ionic-migration and electroosmosis flow caused an increase in lead concentrations movement toward the cathode.

Figures 10 and 11 illustrate the effect of changing tortuosity factor in our model. By increasing tortuosity factor, the pH did not change greatly because the tortuosity had the same effect on proton and hydroxyl velocity (Fig. 10). However, by increasing the tortuosity factor, the movement of lead concentrations in the soil increased and the removal efficiency of lead concentrations increased.

7 Conclusions

We developed an electrokinetic soil remediation model using explicit finite difference method. The summary of our simulation results is as follows:

1. The coefficient of determination (R^2) and index of agreement (IA) between the observed and the predicted pH in electrokinetic soil remediation were 0.987 and 0.976, respectively

2. The coefficient of determination (R^2) and index of agreement (IA) between the observed and the predicted lead concentrations in electrokinetic soil remediation were 0.986 and 0.884, respectively, which indicate that our model predictions are acceptable.

3. According to the result of sensitivity analysis, when retardation factor decreased, it causes improving the model efficiency. When the retardation factor was increased, the EKR for lead removal was retarded.

4. By increasing the electrical field and tortuosity factor, the simulation result indicated increasing the lead removal efficiency in soil. By declining the mentioned parameters, the lead removal efficiency decreased.

References

1. Falamaki A, Tavallali H, Eskandari M, Farahmand SR (2016) Immobilizing some heavy metals by mixing contaminated soils with phosphate admixtures. Int J Civil Eng 14(2):75–81
2. Virkutyle J, Sillanpaa M, Latostebmaa P (2002) Electrokinetic soil remediation-critical overview. Sci Total Environ 289(1–3):97–121
3. Kim SO, Moon SH, Kim KW (2001) Removal of heavy metals from soils using enhanced electrokinetic soil processing. Water Air Soil Pollut 125(1):259–272
4. Vereda-Alonso C, Rodríguez-Maroto JM, García-Delgado RA, Gómez-Lahoz C, García-Herruzo F (2004) Two-dimensional model for soil electrokinetic remediation of heavy metals: application to a copper spiked kaolin. Chemosphere 54:895–903
5. Reddy KR, Claudio C (2009) Electrochemical remediation technologies for polluted soils sediments and groundwater. Wiley, Hoboken
6. Alshawabkeh AN, Acar YB (1996) Electrokinetic remediation. II: theoretical model. J Geotech Eng ASCE 122(3):186–196
7. Haran BS, Popov BN, Zheng G, White RE (1997) Mathematical modeling of hexavalent chromium decontamination of low surface charged soils. J Hazard Mater 55(1–3):93–107
8. Jacobs RA, Sengun MZ, Hicks RE, Probstein RF (1994) Model and experiments on soil remediation by electric fields. J Environ Sci Health Part A Environ Sci Eng Toxicol 29(9):1933–1955
9. Kim SO, Kim JJ, Yun ST, Kim KW (2003) Numerical and experimental studies on cadmium (II) transport in kaolinite clay under electrical fields. Water Air Soil Pollut 150(1–4):135–162
10. Kim SO, Kim JJ, Kim KW, Yun ST (2004) Models and experiments on electrokinetic removal of Pb(II) from kaolinite clay. Sep Sci Technol 39(8):1927–1951
11. Park Jin-Soo, Kim Soon-Oh, Kim Kyoung-Woong, Kim BR, Moon S-H (2003) Numerical analysis for electrokinetic soil processing enhanced by chemical conditioning of the electrode reservoirs. J Hazard Mater 99(1):71–85
12. Hafiz A (2004) Evaluation and enhancement of electro-kinetic technology for remediation of chromium copper arsenic from clayey soil. PhD thesis, Florida state University
13. Mascia M, Palmas S, Polcaro AM, Vacca A, Muntoni A (2007) Experimental study and mathematical model on remediation of Cd spiked kaolinite by electrokinetics. Electrochim Acta 52:3360–3365
14. Al-Hamdan AZ, Reddy KR (2008) Electrokinetic Remediation Modeling Incorporating Geochemical Effects. J Geotech Geoenviron Eng 134(1):91–105
15. Yeung AT, Hsu CN, Menon RM (2011) Electrokinetic extraction of lead from kaolinites: I. Numerical modeling. Environmentalist 31:26–32
16. Ghasemzadeh H (2008) Heat and contaminant transport in unsaturated soil. Int J Civil Eng 6(2):90–107
17. Mitchell JK (1993) Fundamentals of soil behavior, 2nd edn. Wiley, New York
18. Eykholt GR, Daniel DE (1994) Impact of system chemistry on electroosmosis in contaminated soil. J Geotech Eng 120(5):797–815
19. Paz-García JM, Johannesson B, Ottosen LM, Ribeiro AB, Rodríguez-Maroto JM (2011) Modeling of electrokinetic processes by finite element integration of the Nernst–Planck–Poisson system of equations. Sep Purif Technol 79:183–192
20. Lorenz PB (1969) Surface conductance and electrokinetic properties of kaolinite beds. Clays Clay Miner 17:223–231
21. Alshawabkeh AN (1994) Theoretical and experimental modeling of removing contaminants from soils by an electric field. PhD thesis, The Louisiana State University, Baton Rouge, LA, USAs
22. Daniel DE (1993) Geotechnical practice for waste disposal. Chapman & Hall, London
23. Yong RN, Warkentin BP, Phadungchewit Y, Galvez R (1990) Buffer capacity and lead retention in some clay materials. Water Air Soil Pollut 53(1):53–67
24. Cao X (1997) Modeling electrokinetically enhanced transport of multispecies in porous media under transient electrical field. MSc thesis, Lehigh University, Bethlehem, PA, USA
25. Wilkowe A (1992) A modified finite difference model of electrokinetic transport in porous media. Master of Science thesis, Lehigh University
26. Asadi A, Huat BBK, Moayedi H, Shariatmadari N, Parsaie A (2011) Electro-osmotic permeability coefficient of peat with different degree of humification. Int J Electrochem Sci 6(11):4481–4492
27. Lide DR (2010) CRC handbook of chemistry and physics: a ready-reference book of chemical and physical data. CRC Press, Boca Raton
28. Acar YB, Robert JG, Akram AN, Marks RE, Puppala S, Bricka M, Parker R (1995) Electrokinetic technology: basis and technology status. J Hazard Mater 40(2):117–137